**Supporting Information:**

# Hierarchical porous carbon nanospheres for efficient removal of toxic organic water contaminants of phenol and methylene blue

Sukanya Kundu, Ipsita Hazra Chowdhury and Milan Kanti Naskar*

Sol-Gel Division, Council of Scientific and Industrial Research-Central Glass and Ceramic Research Institute, Kolkata 700 032, India

*Corresponding author: Ph: +91 33 2473 3496 (Ext. 3516), E-mail: milan@cgcri.res.in

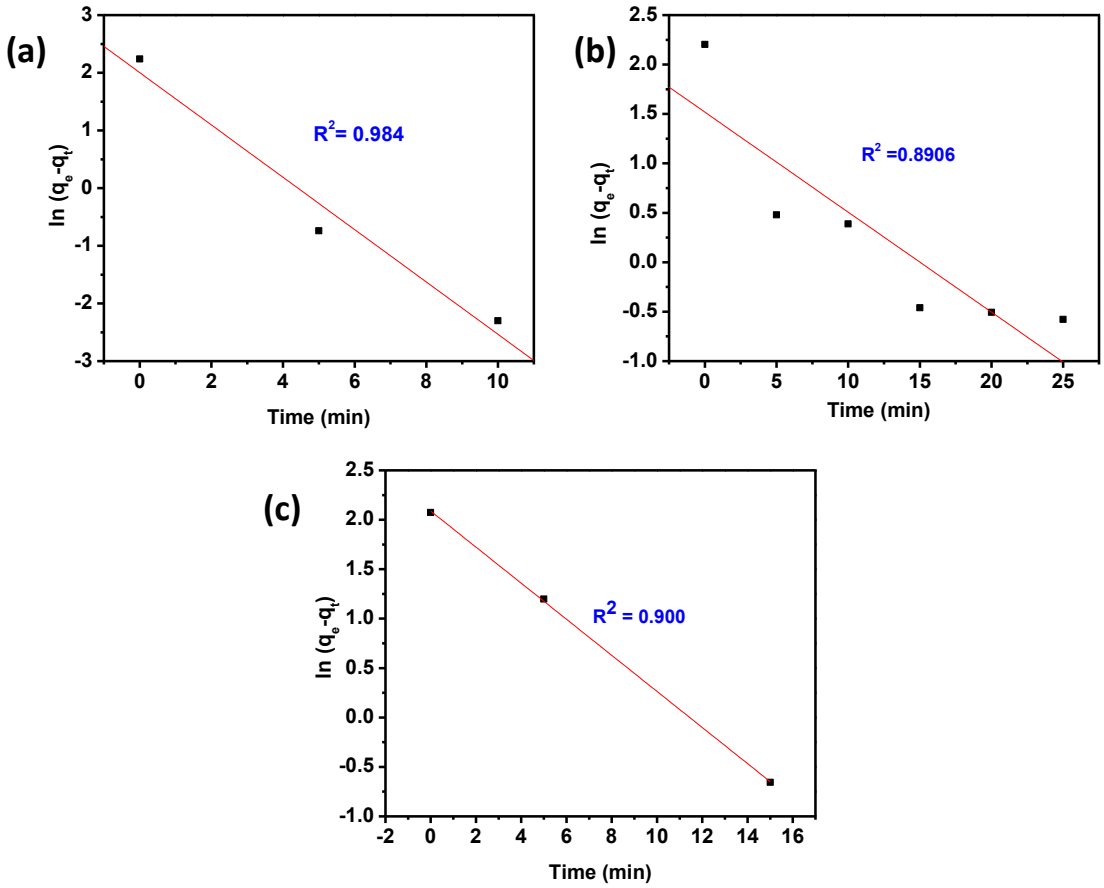


Fig. S1: Pseudo-first order kinetic plots for the adsorption of phenol by porous carbon nanopheres: (a) CF108, (b) CF127 and (c) CL64.

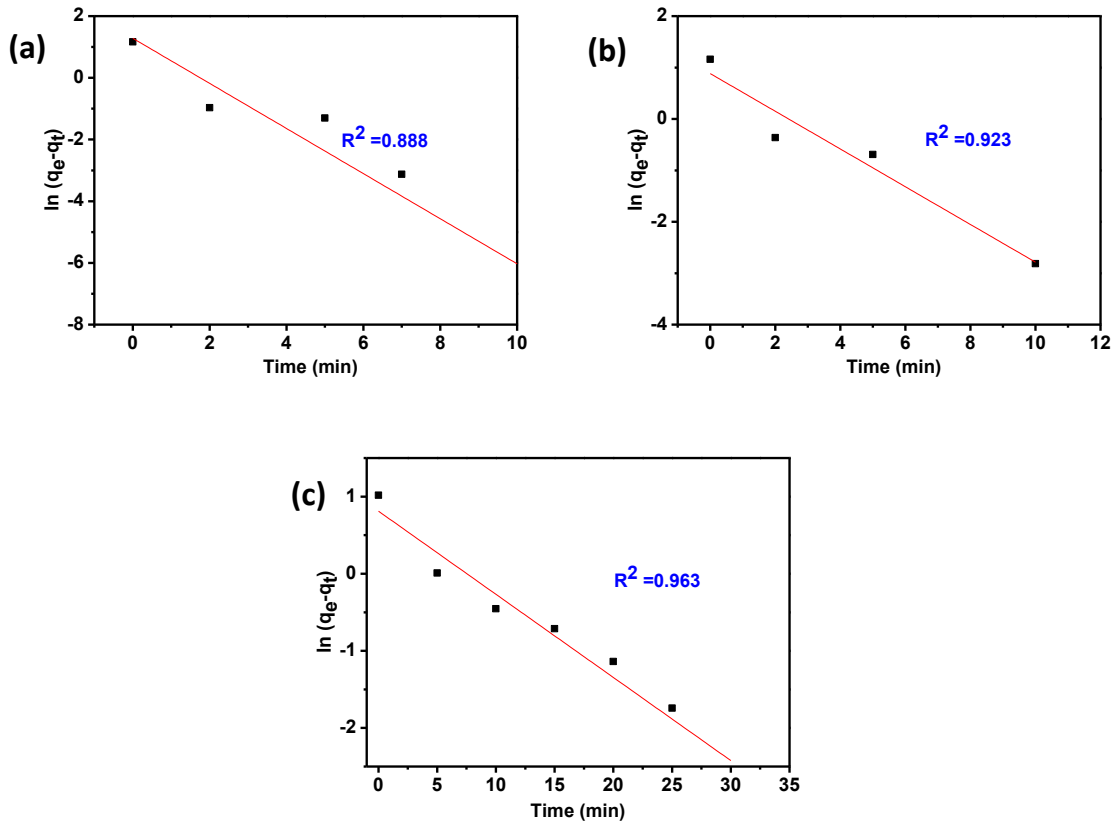


Fig. S2: Pseudo-first order kinetic plots for the adsorption of MB by porous carbon nanopheres: (a) CF108, (b) CF127 and (c) CL64.

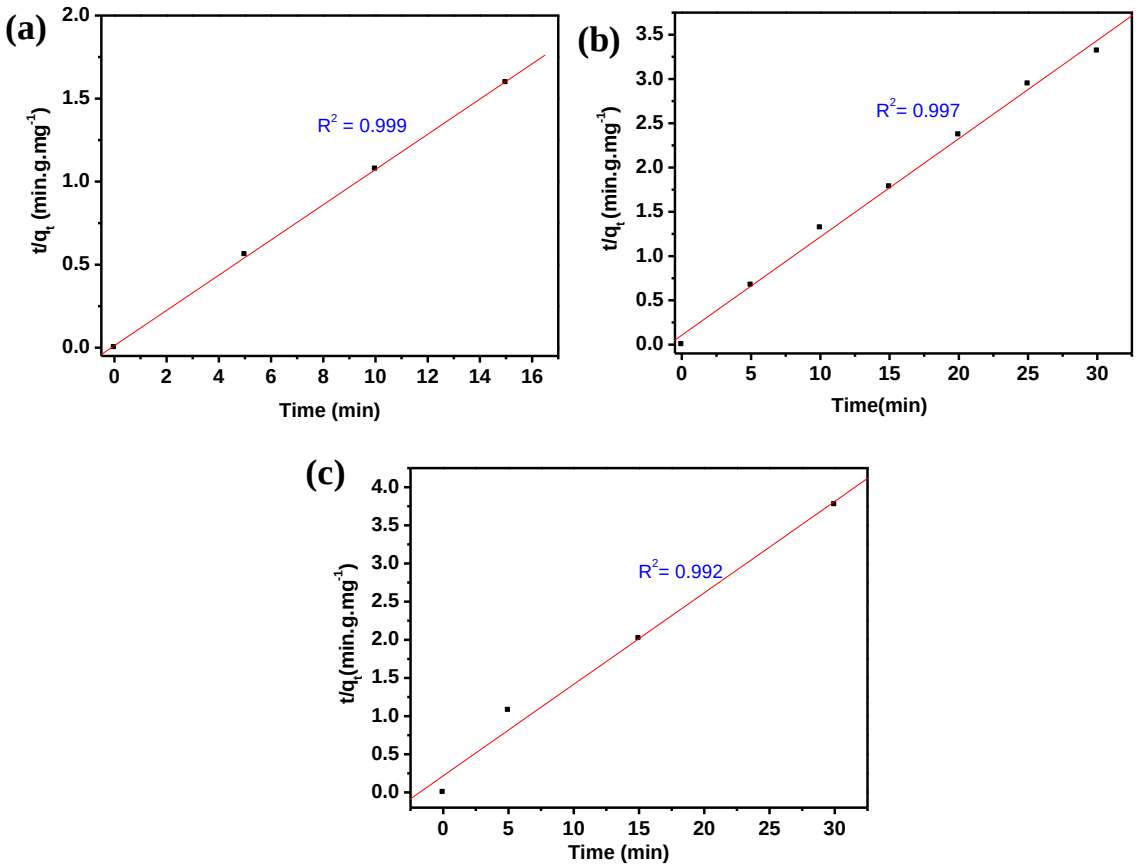


Fig. S3: Pseudo-second order kinetic plots for the adsorption of phenol by porous carbon nanopheres: (a) CF108, (b) CF127 and (c) CL64.

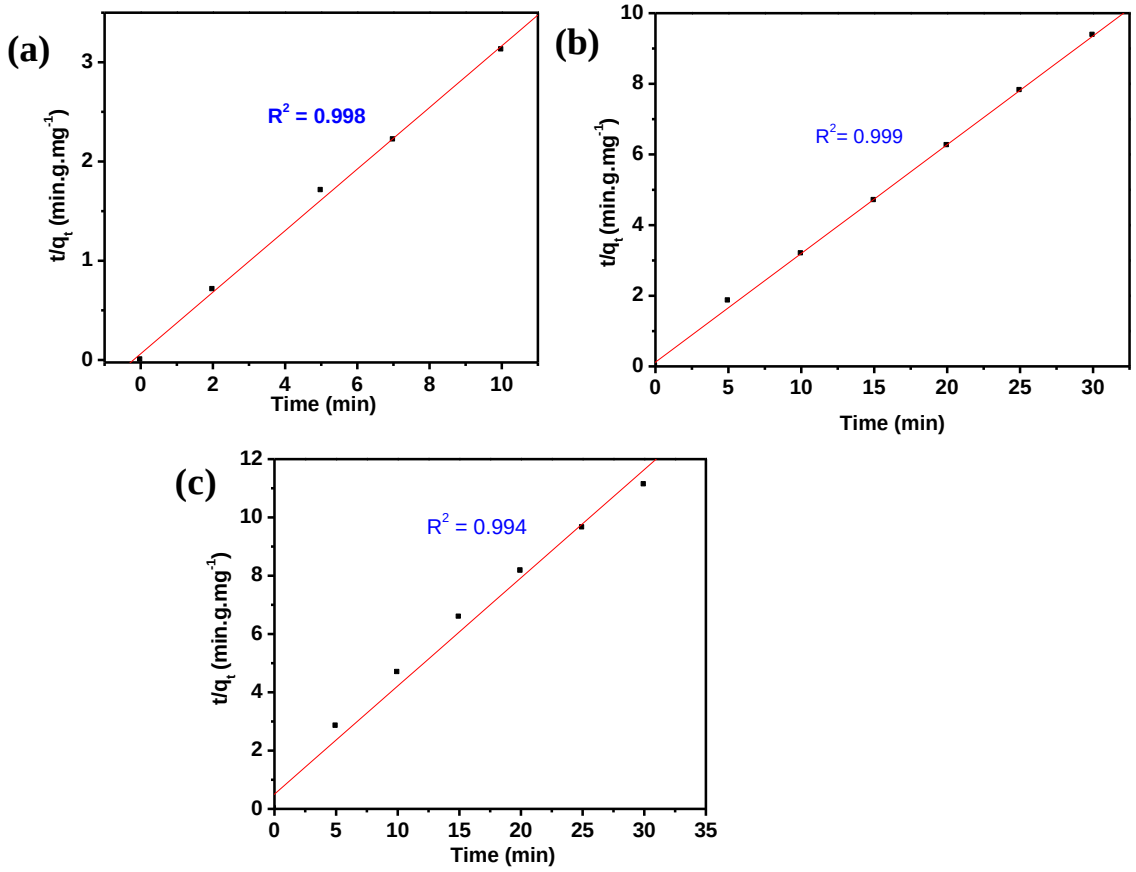


Fig. S4: Pseudo-second order kinetic plots for the adsorption of MB by the porous carbon nanopheres: (a) CF108, (b) CF127 and (c) CL64.

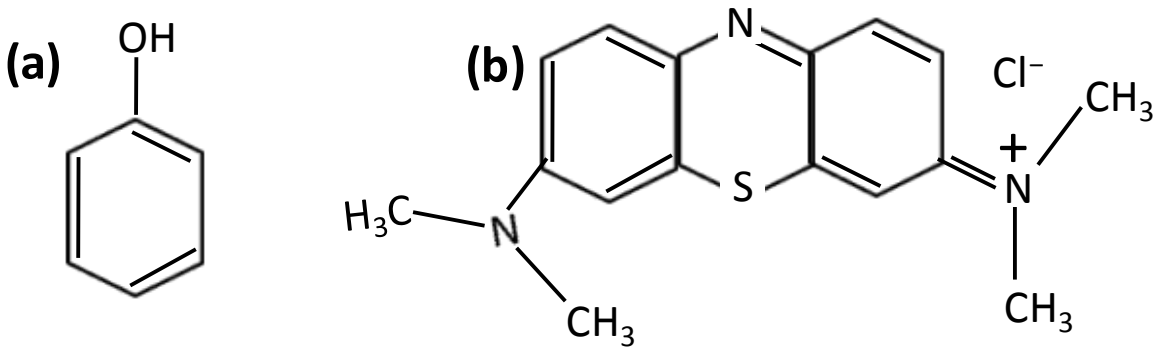


Fig. S5: Structure of (a) phenol and (b) methylene blue (MB).

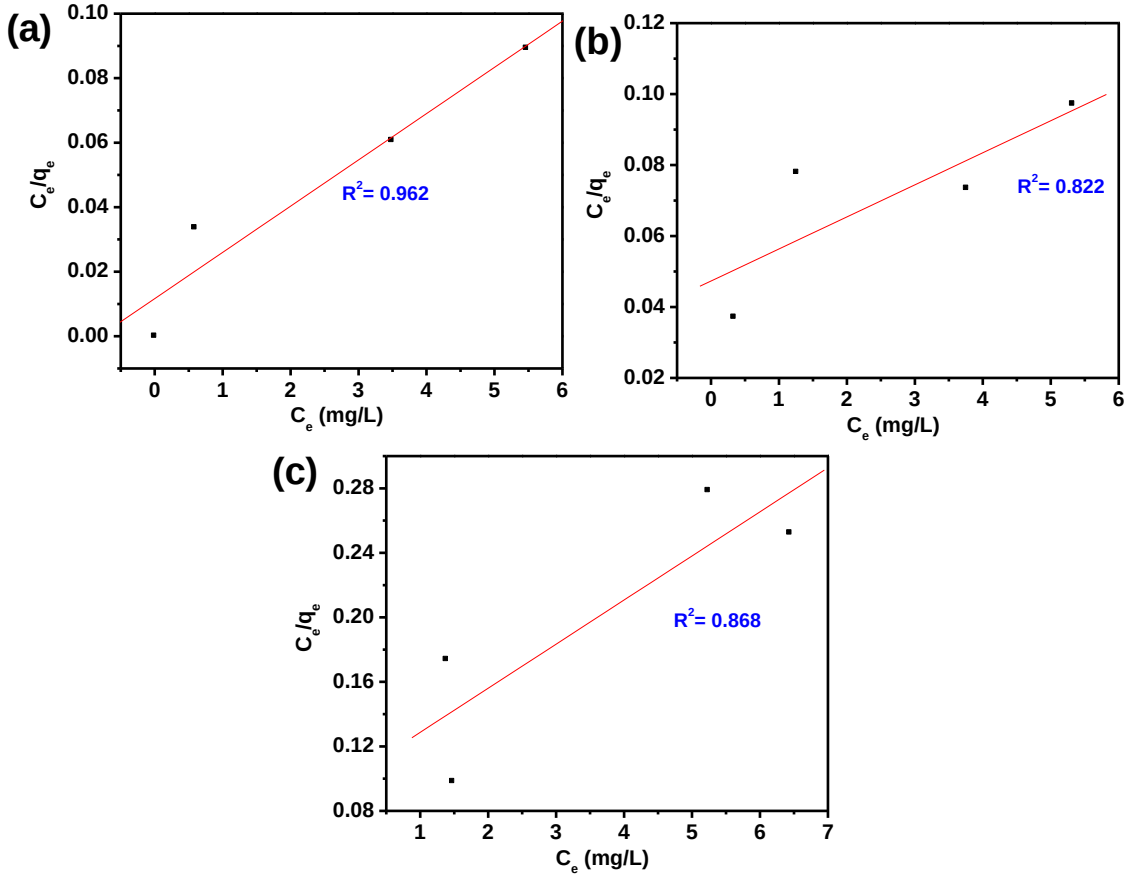


Fig. S6: Langmuir isotherms for phenol adsorption on the porous carbon nanopheres with different adsorbent doses: (a) CF108, (b) CF127 and (c) CL64.

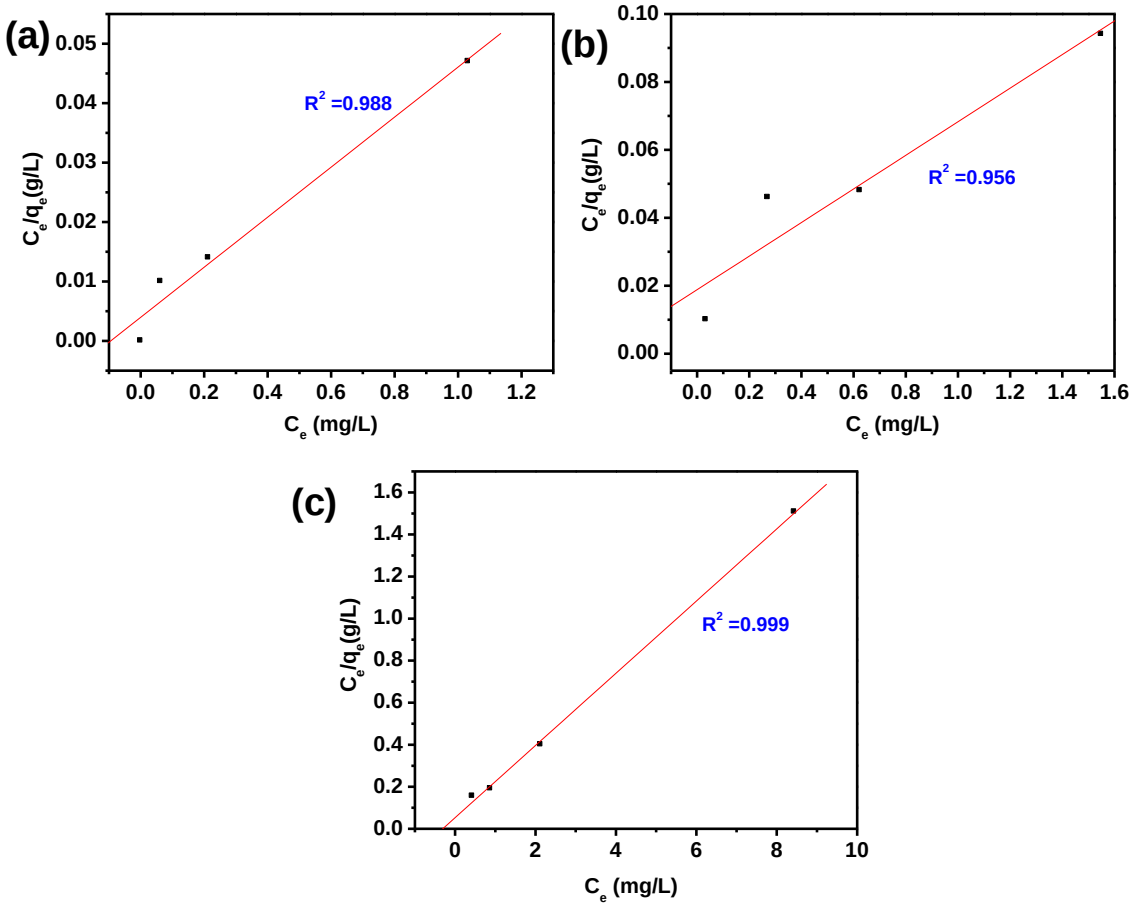


Fig. S7: Langmuir isotherms for MB adsorption on the porous carbon nanopheres with different adsorbent doses: (a) CF108, (b) CF127 and (c) CL64.

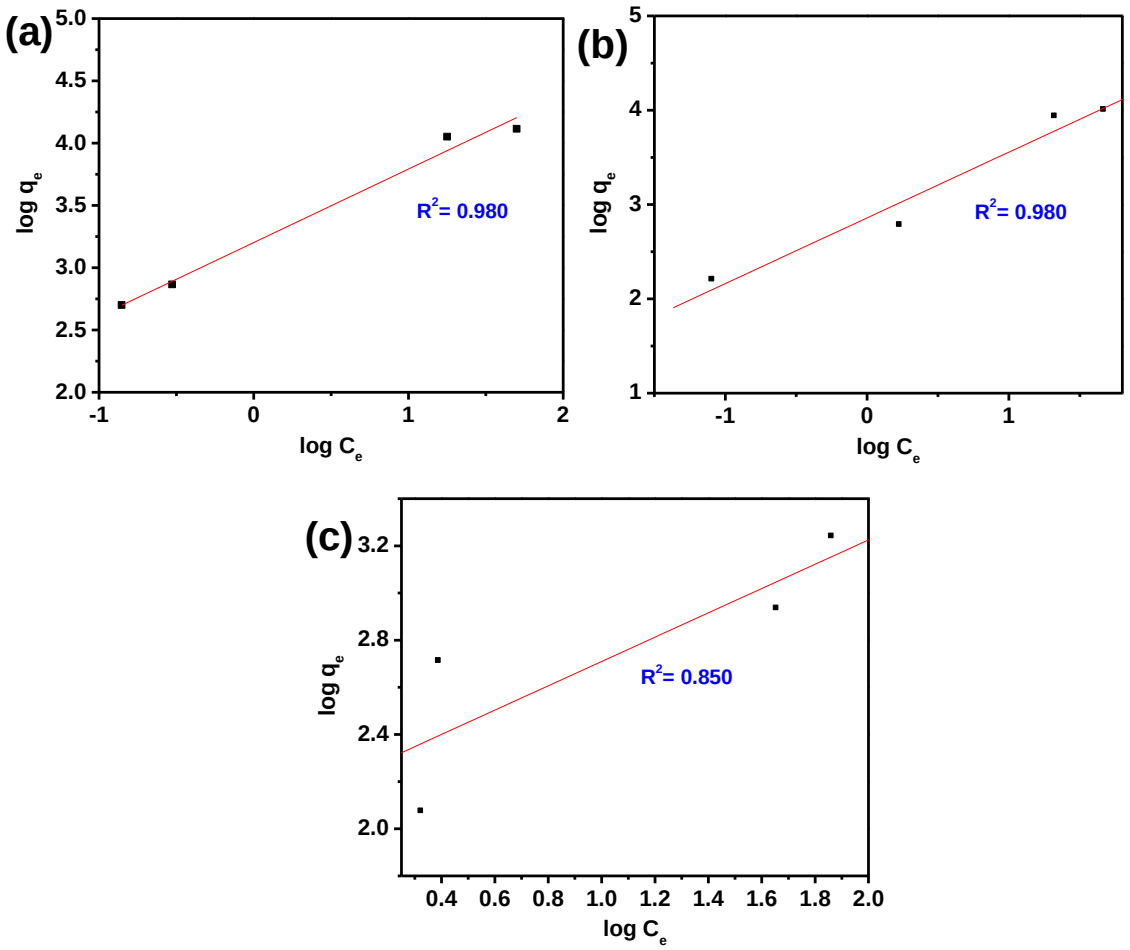


Fig. S8: Freundlich isotherms for phenol adsorption on the porous carbon nanopheres with different adsorbent doses: (a) CF108, (b) CF127 and (c) CL64.

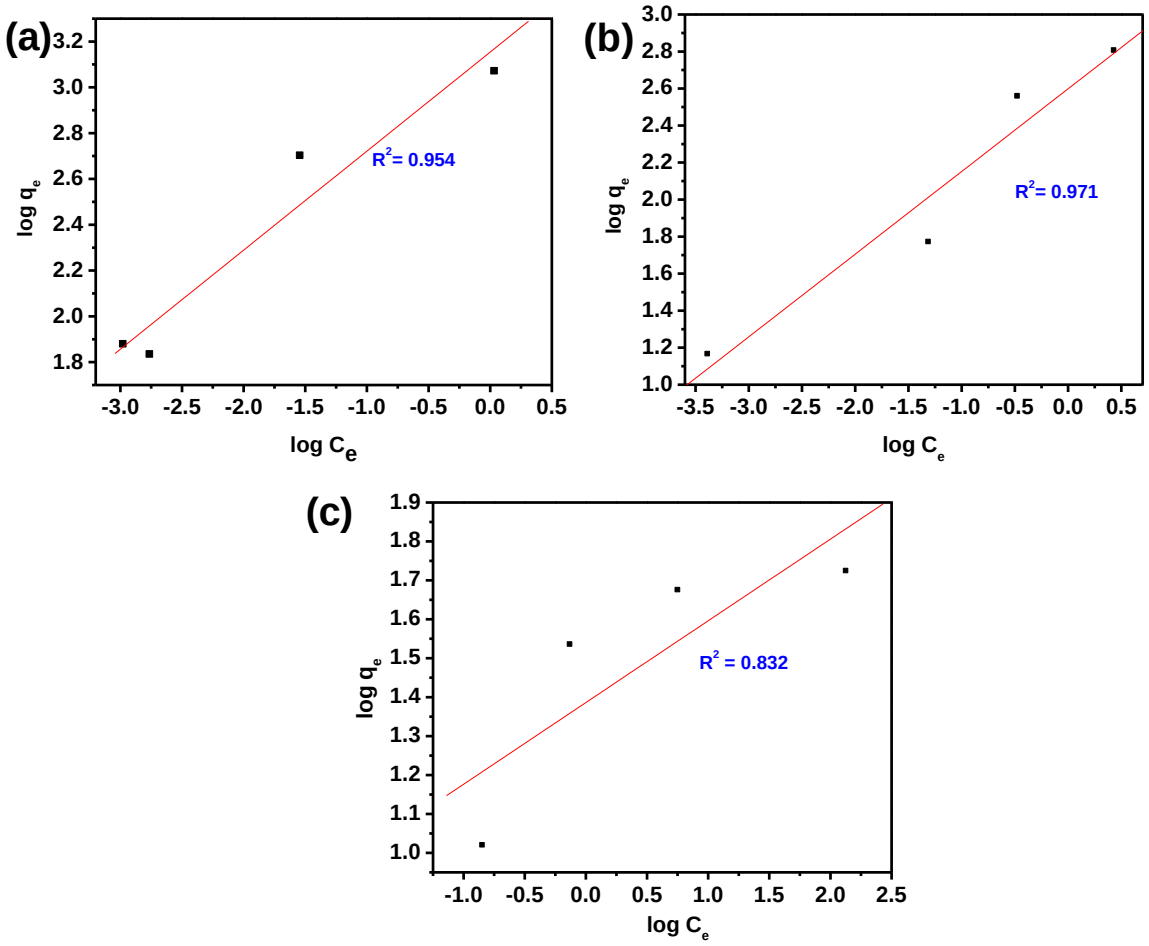


Fig. S9: Freundlich isotherms for MB adsorption on the porous carbon nanopheres with different adsorbent doses: (a) CF108, (b) CF127 and (c) CL64.

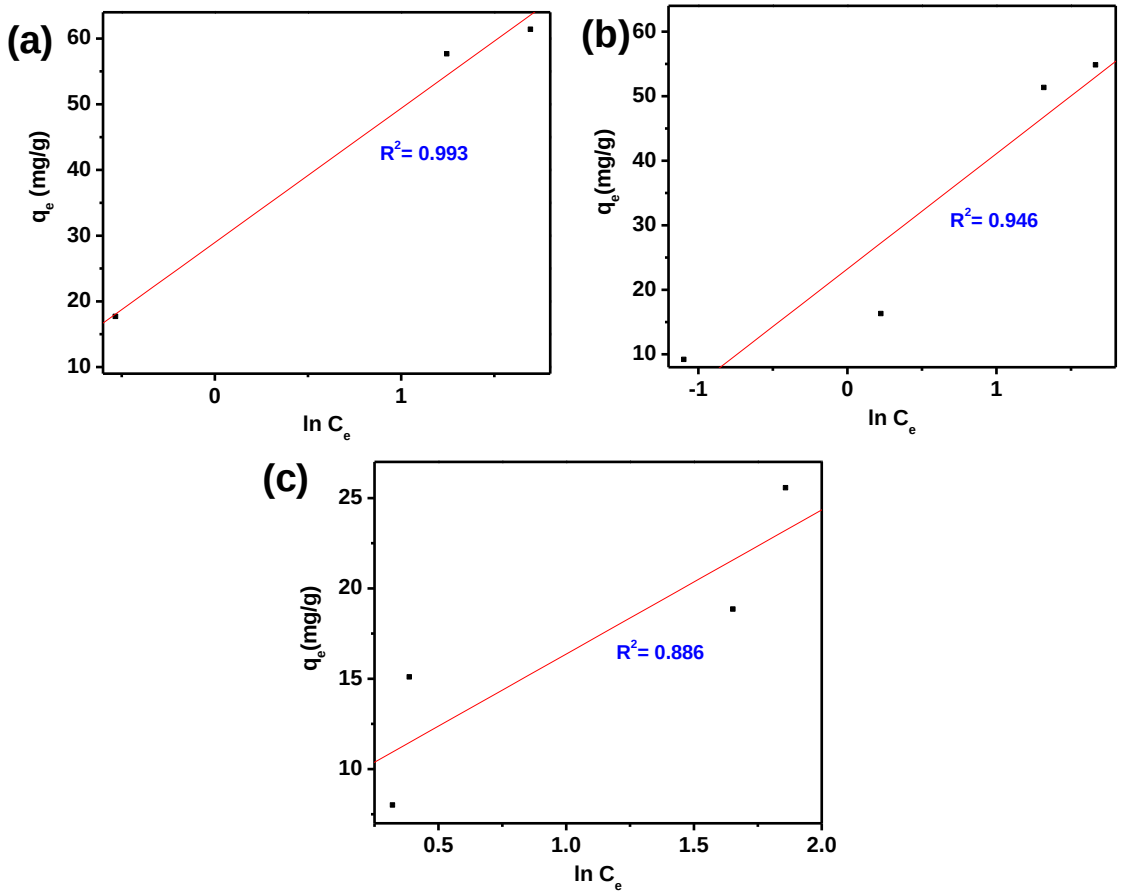


Fig. S10: Temkin isotherms for phenol adsorption on the porous carbon nanopheres with different adsorbent doses: (a) CF108, (b) CF127 and (c) CL64.

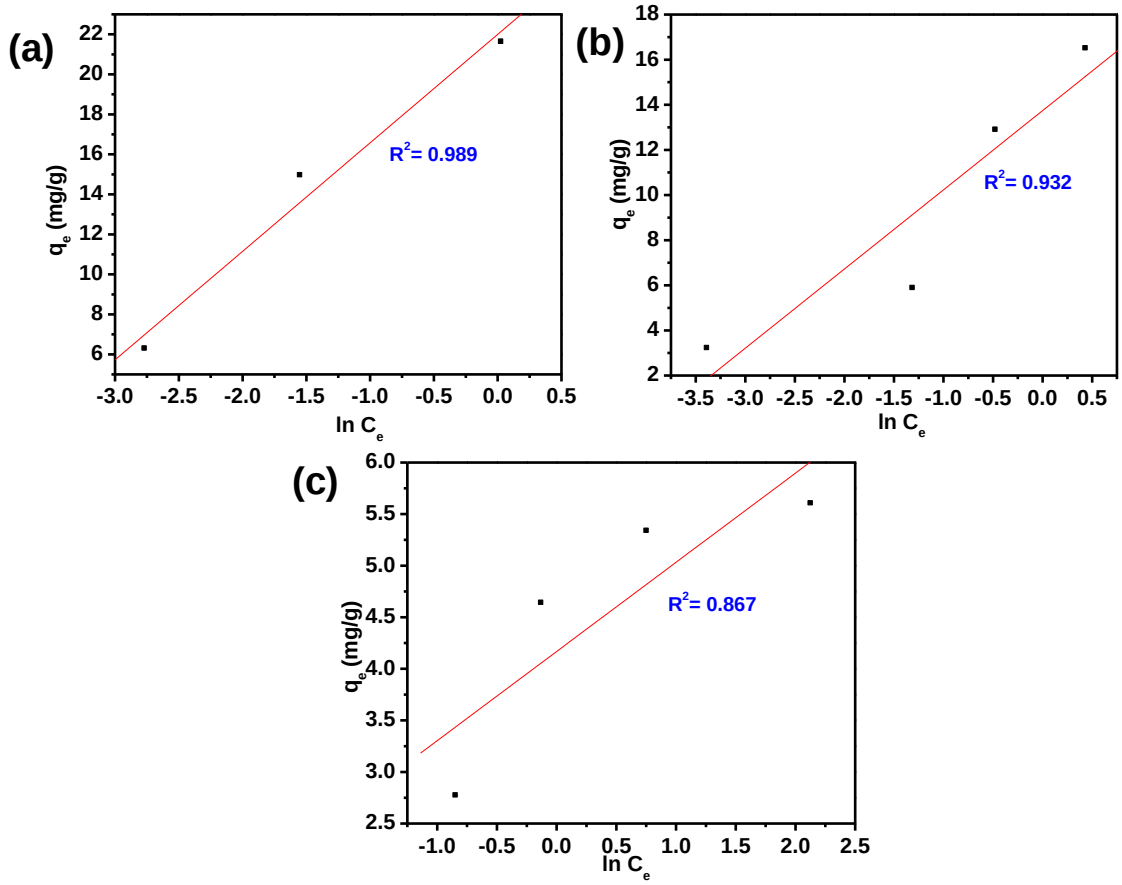


Fig. S11: Temkin isotherms for MB adsorption on the porous carbon nanopheres with different adsorbent doses: (a) CF108, (b) CF127 and (c) CL64.

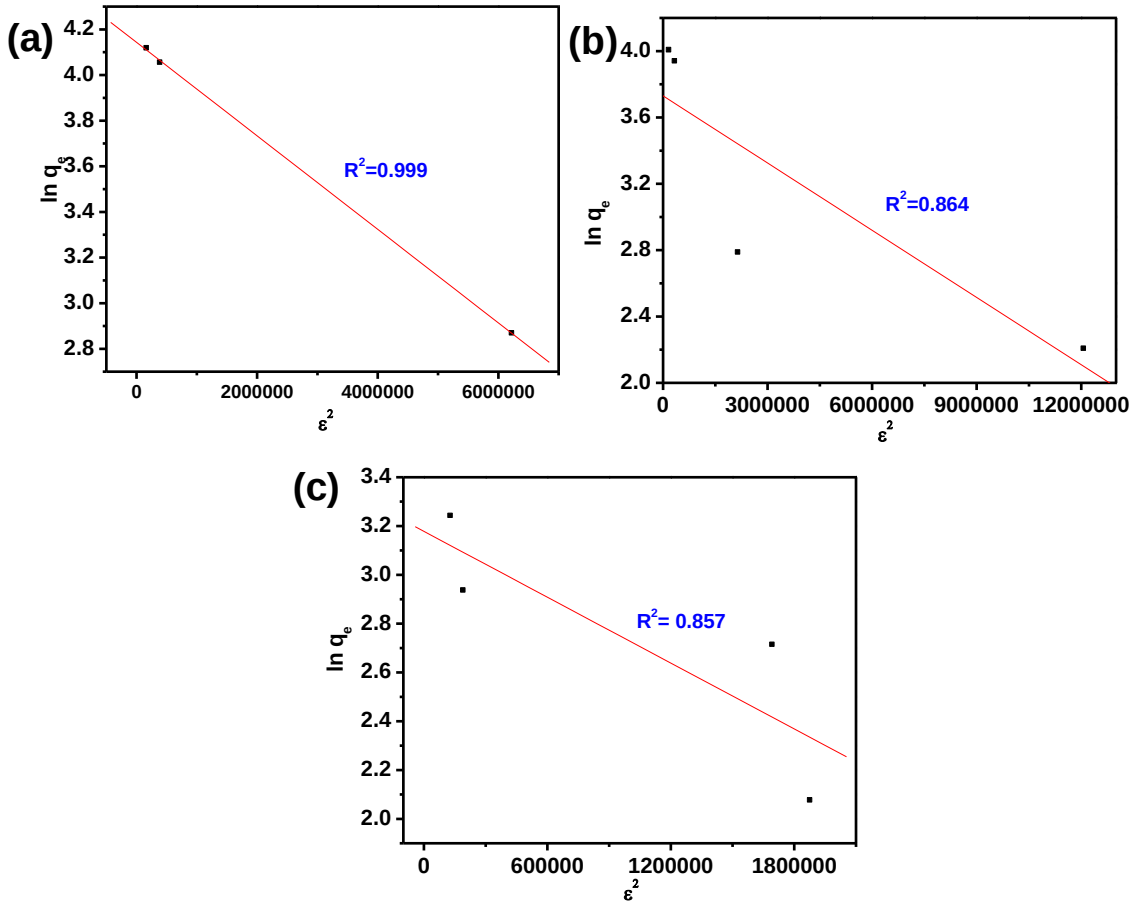


Fig. S12: Dubinin–Radushkevich isotherms for phenol adsorption on the porous carbon nanopheres with different adsorbent doses: (a) CF108, (b) CF127 and (c) CL64.

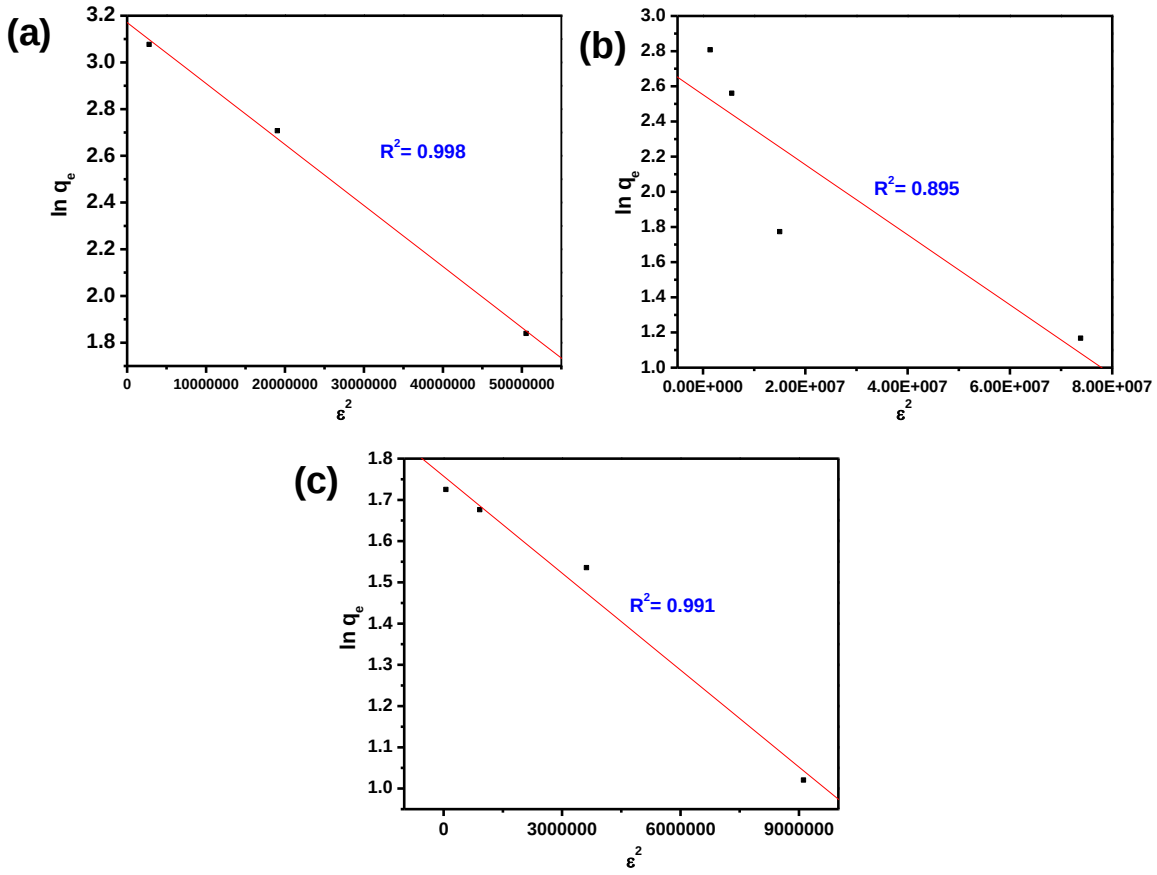


Fig. S13: Dubinin–Radushkevich isotherms for MB adsorption on the porous carbon nanopheres with different adsorbent doses: (a) CF108, (b) CF127 and (c) CL64.

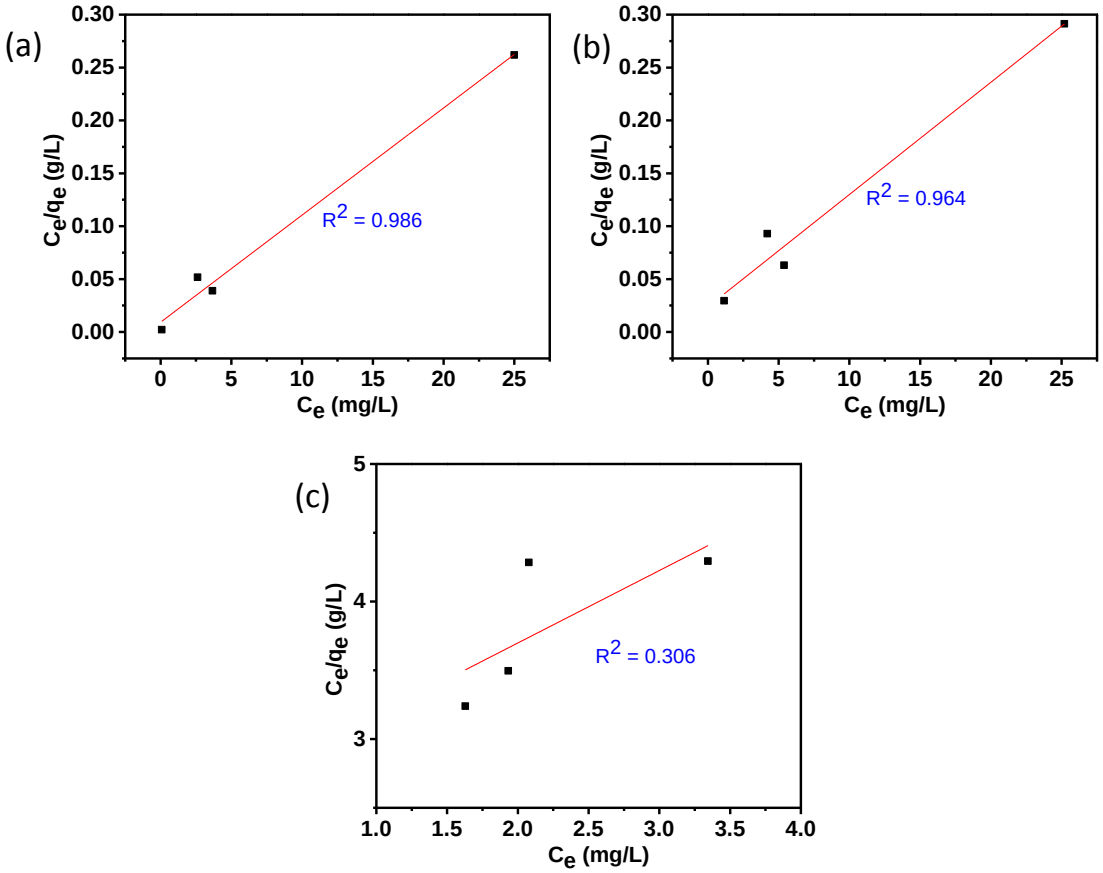


Fig. S14: Langmuir isotherms for phenol adsorption on the porous carbon nanopheres with different adsorbate concentration :(a) CF108, (b) CF127 and (c) CL64.

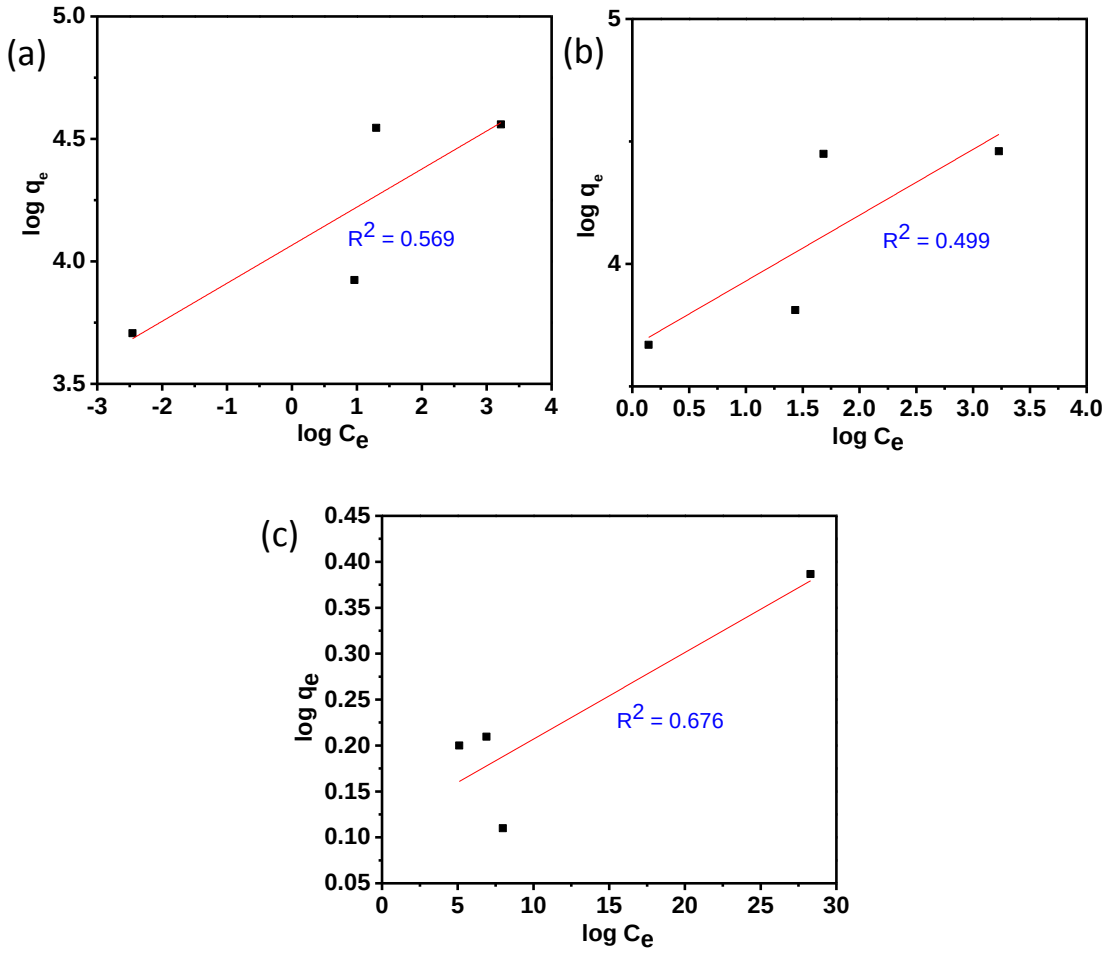


Fig. S15: Freundlich isotherms for phenol adsorption on the porous carbon nanopheres with different adsorbate concentration :(a) CF108, (b) CF127 and (c) CL64.

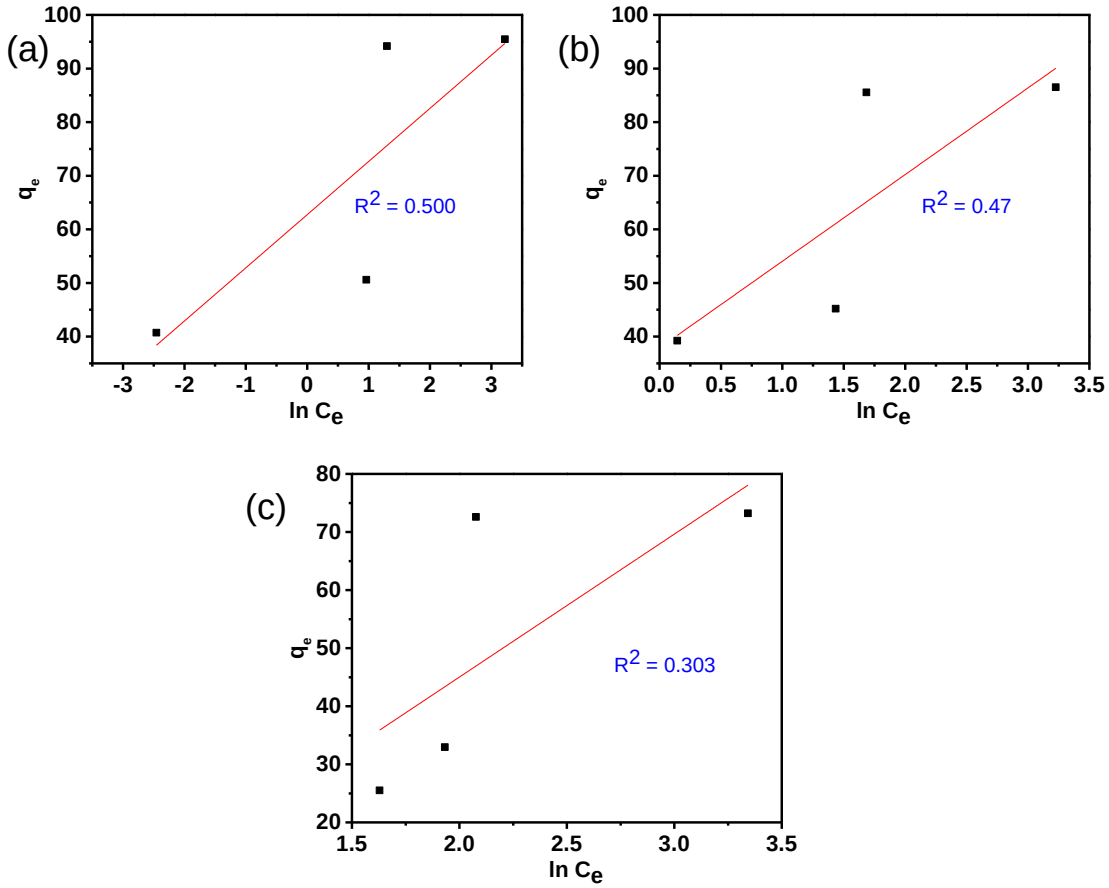


Fig. S16: Temkin isotherms for phenol adsorption on the porous carbon nanopheres with different adsorbate concentration :(a) CF108, (b) CF127 and (c) CL64.

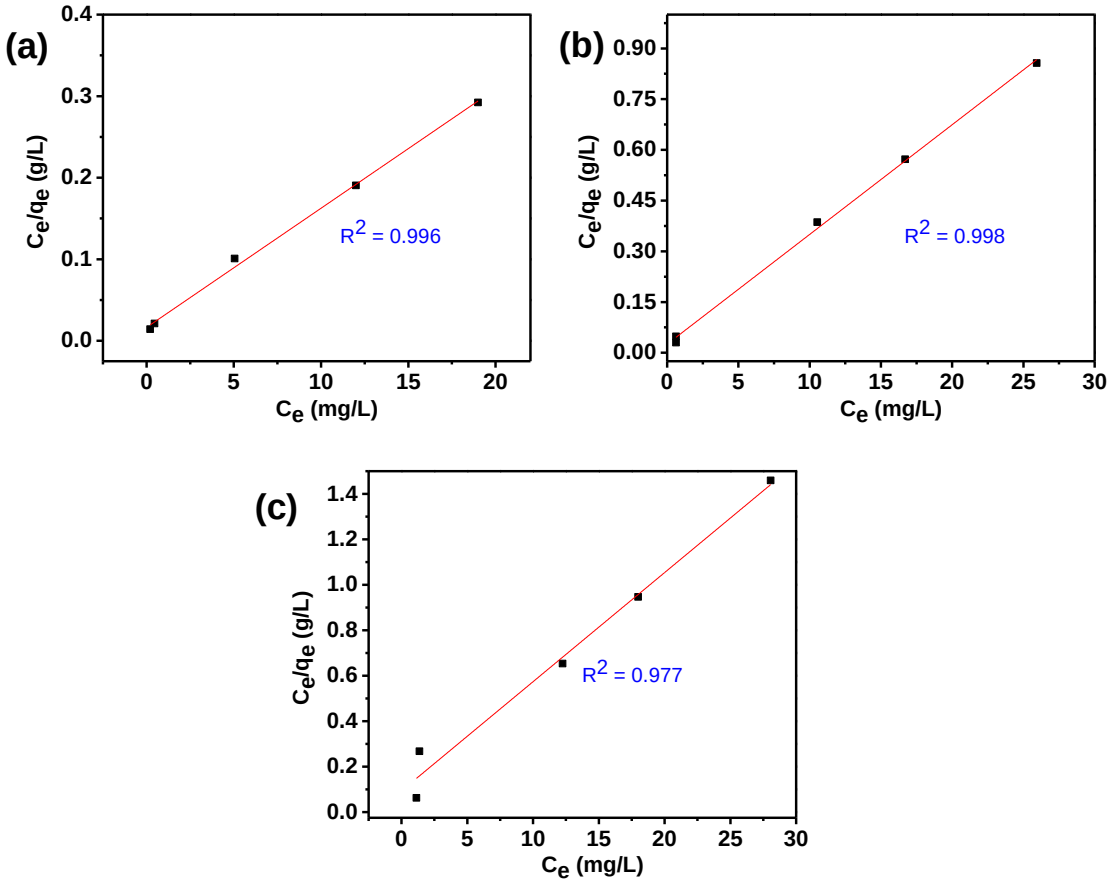


Fig. S17: Langmuir isotherms for MB adsorption on the porous carbon nanopheres with different adsorbate concentration :(a) CF108, (b) CF127 and (c) CL64.

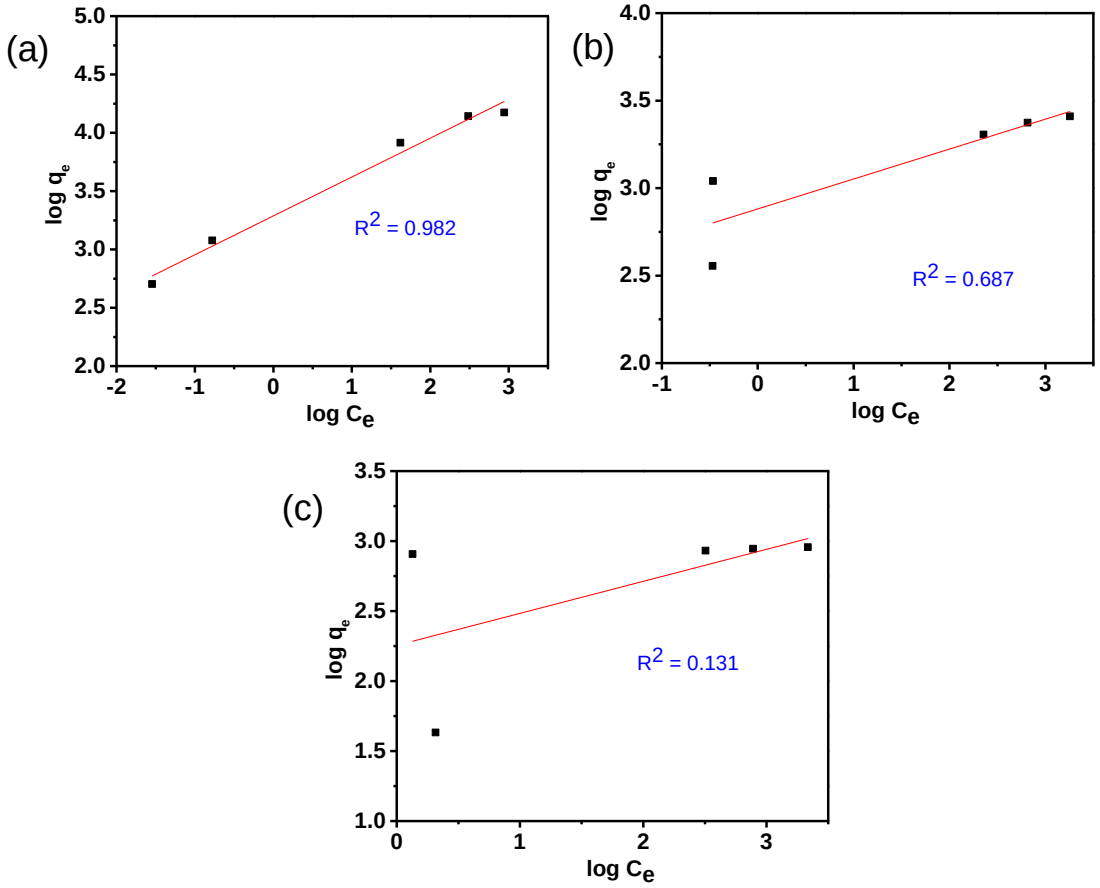


Fig. S18: Freundlich isotherms for MB adsorption on the porous carbon nanopheres with different adsorbate concentration :(a) CF108, (b) CF127 and (c) CL64.

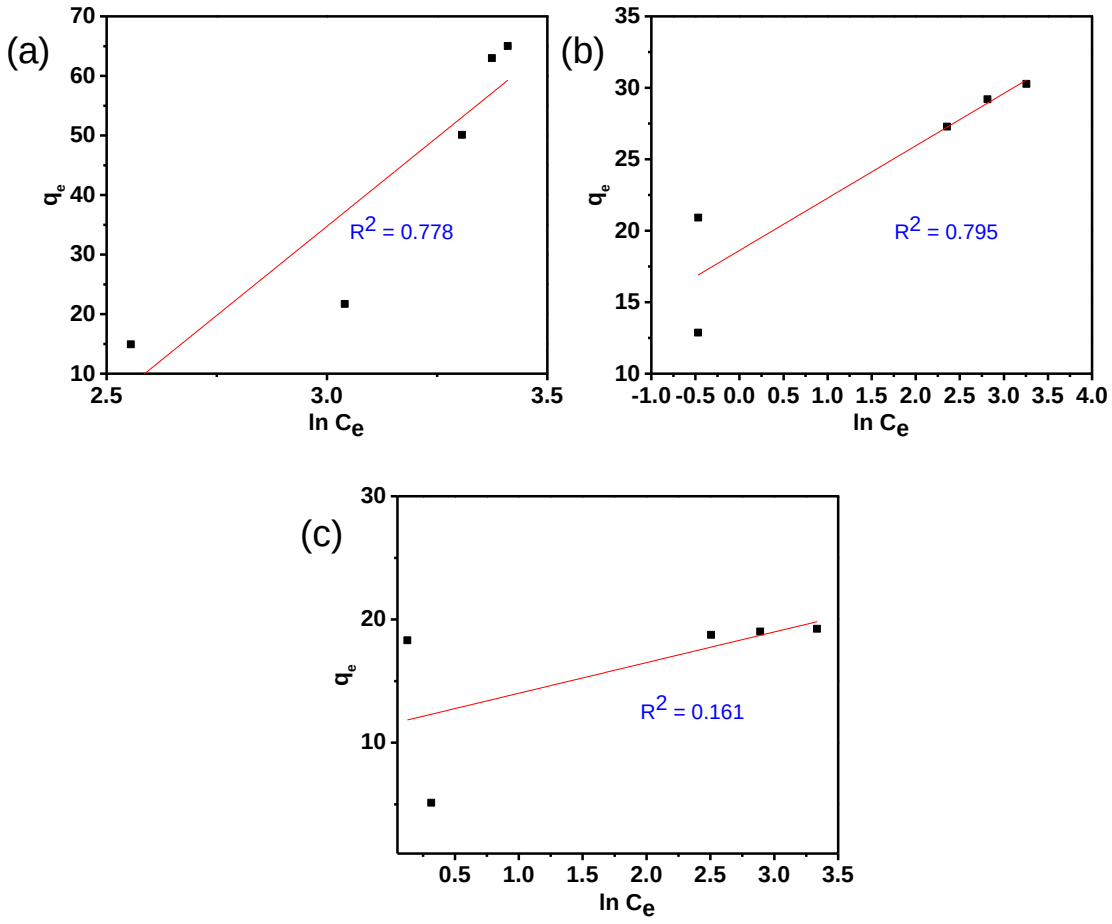


Fig. S19: Temkin isotherms for MB adsorption on the porous carbon nanopheres with different adsorbate concentration :(a) CF108, (b) CF127 and (c) CL64.

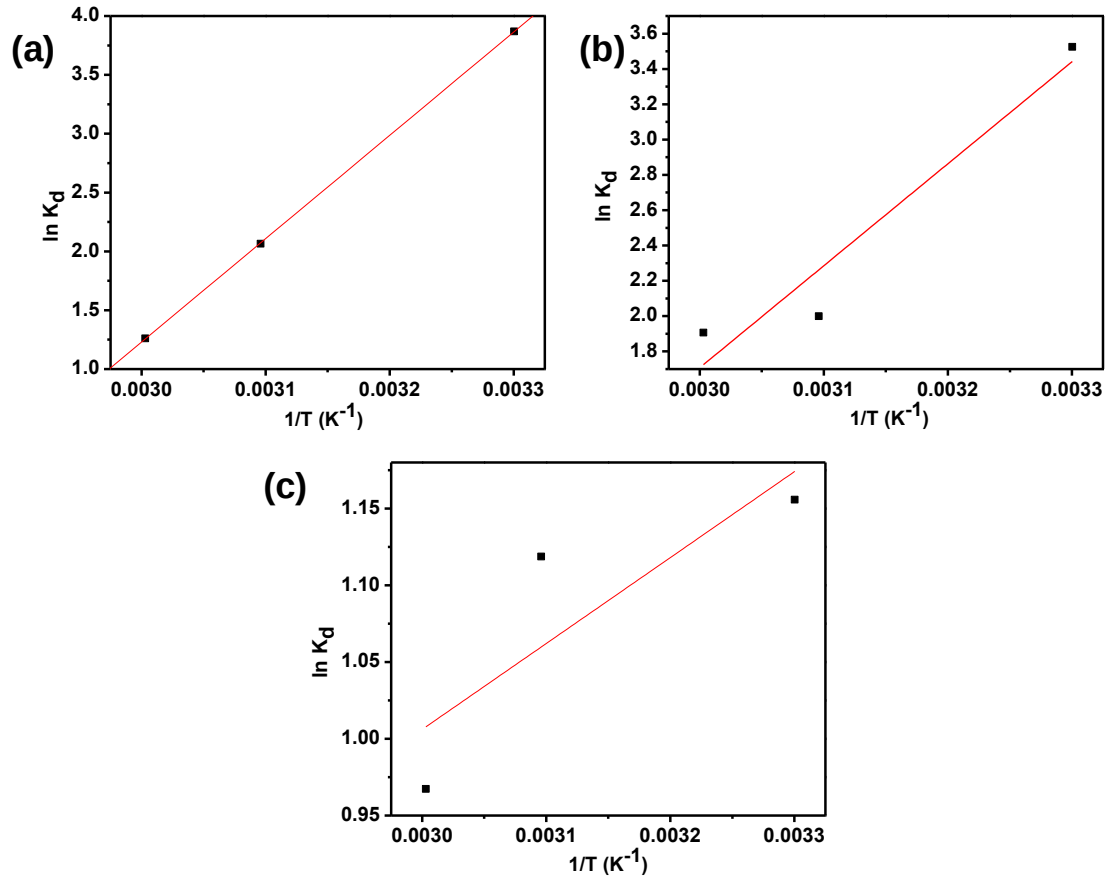


Fig. S20: Plot of ln $K_d$ versus 1/T for phenol adsorption on the porous carbon nanopheres:(a) CF108, (b) CF127 and (c) CL64.

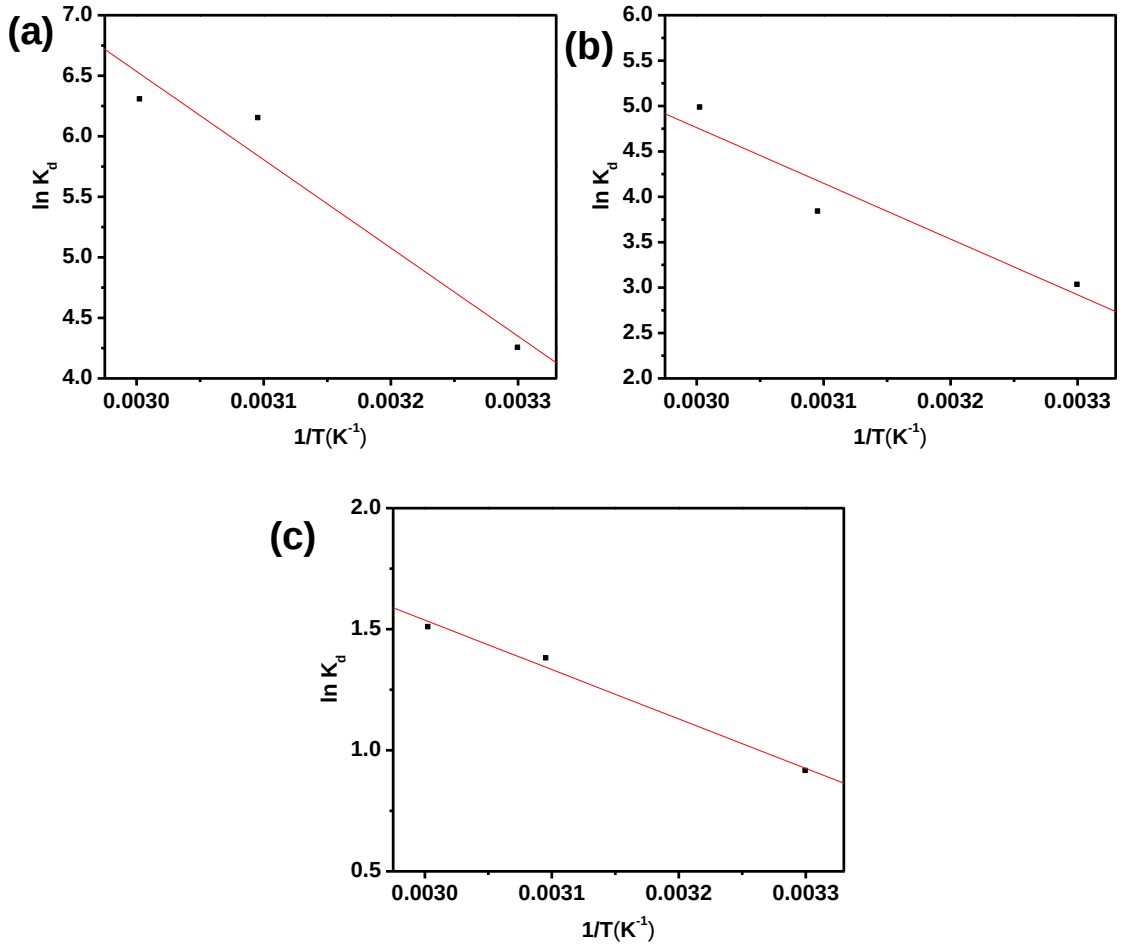


Fig. S21: Plot of ln $K_d$ versus 1/T for MB adsorption on the porous carbon nanopheres:(a) CF108, (b) CF127 and (c) CL64.

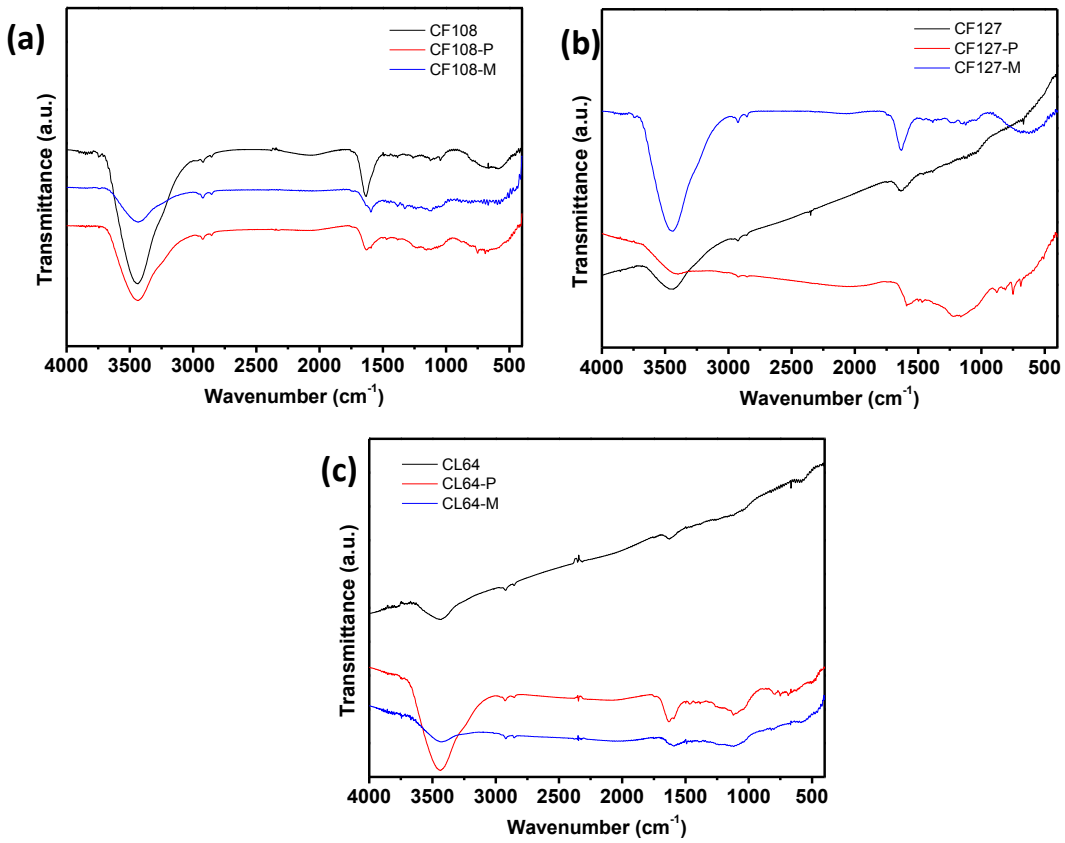


Fig. S22: FTIR spectra of porous carbon nanospheres before adsorption ((a) CF108, (b) CF127 and (c) CL64), after phenol adsorption ((a) CF108-P, (b) CF127-P and (c) CL64-P) and MB adsorption ((a) CF108-M, (b) CF127-M and (c) CL64-M).

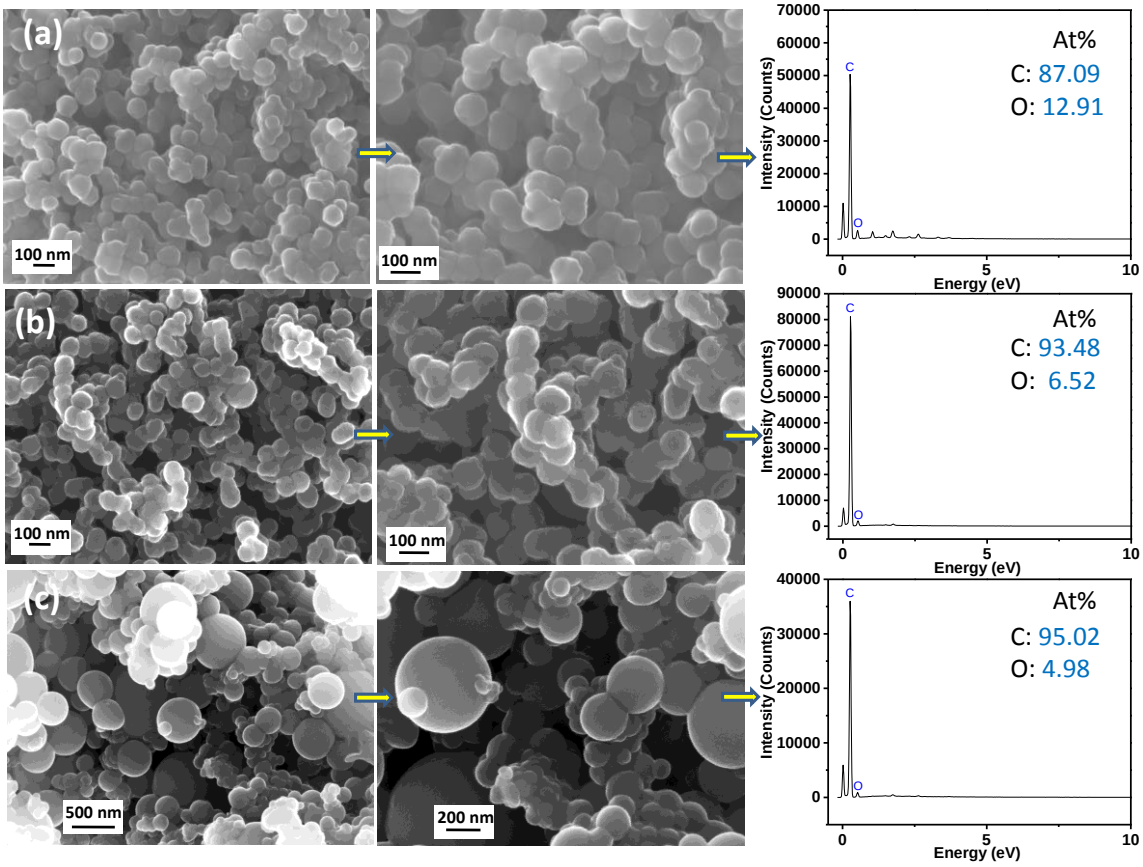


Fig. S23: FESEM images (low and high magnification) and EDX analysis of the samples (a) CF108-P, (b) CF127-P and (c) CL64-P after adsorption of phenol.

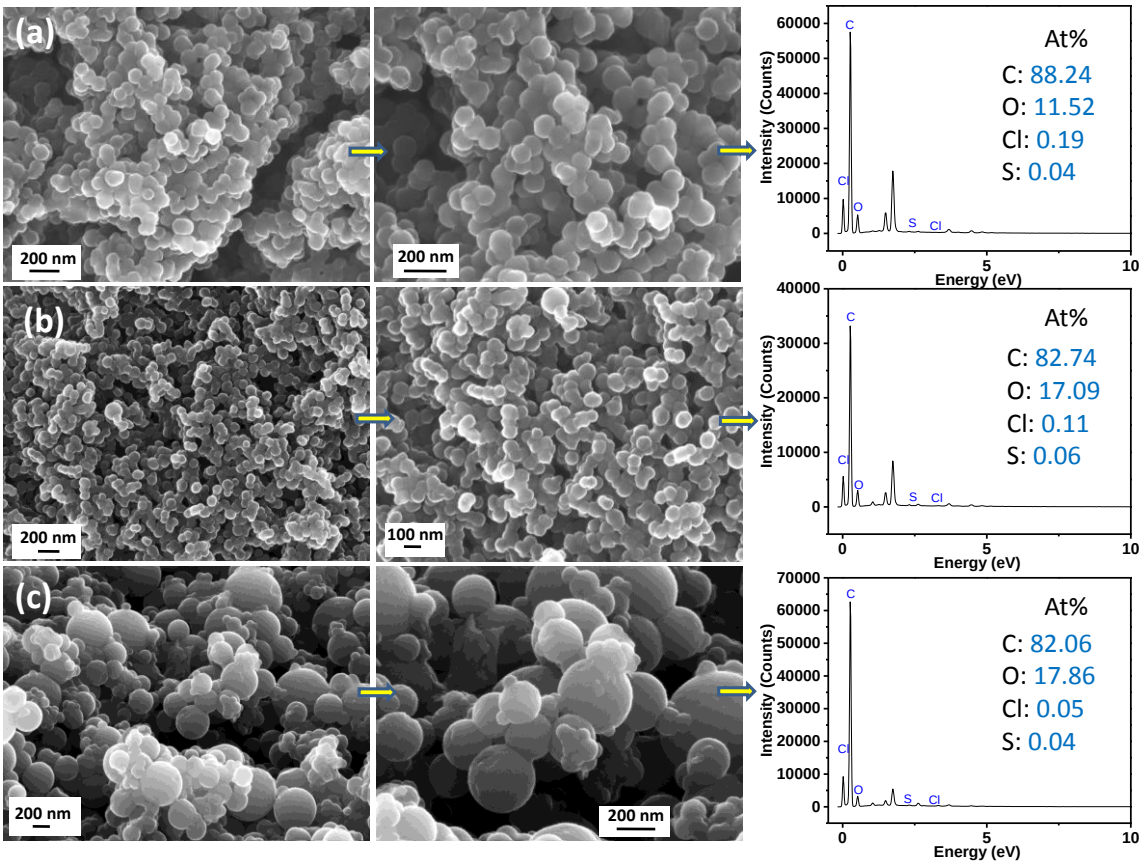


Fig. S24: FESEM images (low and high magnification) and EDX analysis of the samples (a) CF108-M, (b) CF127-M and (c) CL64-M after adsorption of MB.

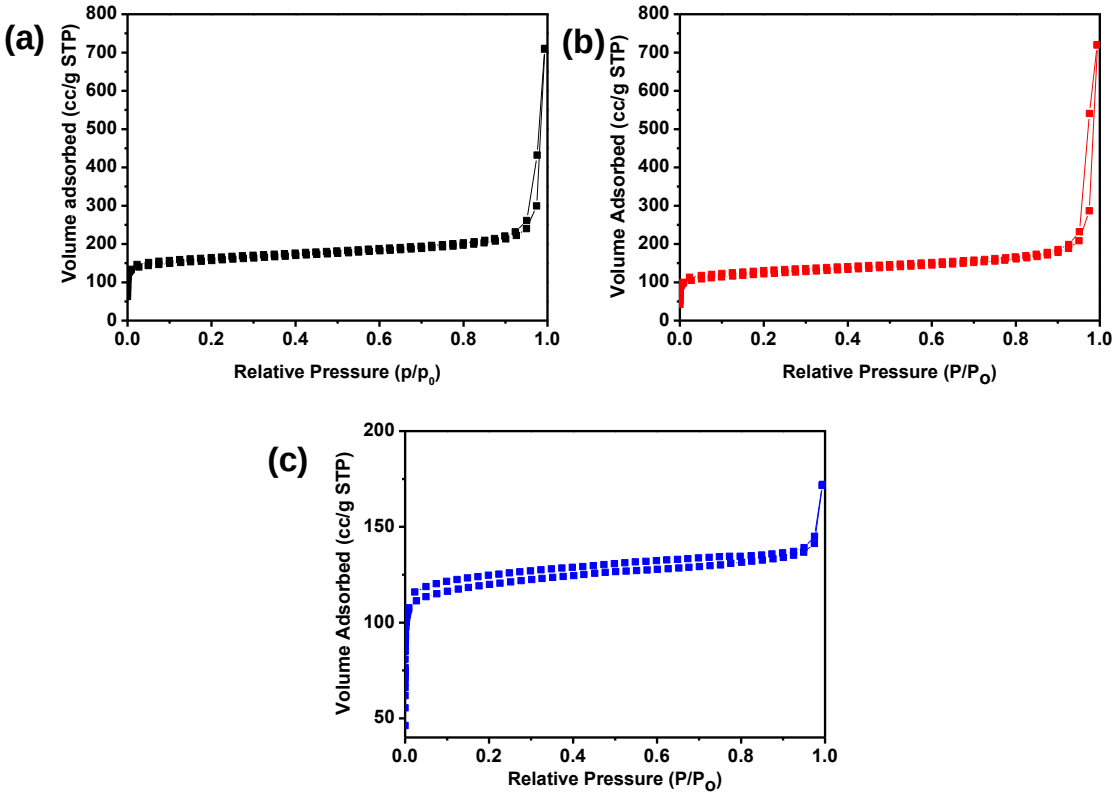


Fig. S25: $N_2$ adsorption-desorption isotherms of porous carbon nanospheres after phenol adsorption: (a) CF108-P, (b) CF127-P and (c) CL64-P.

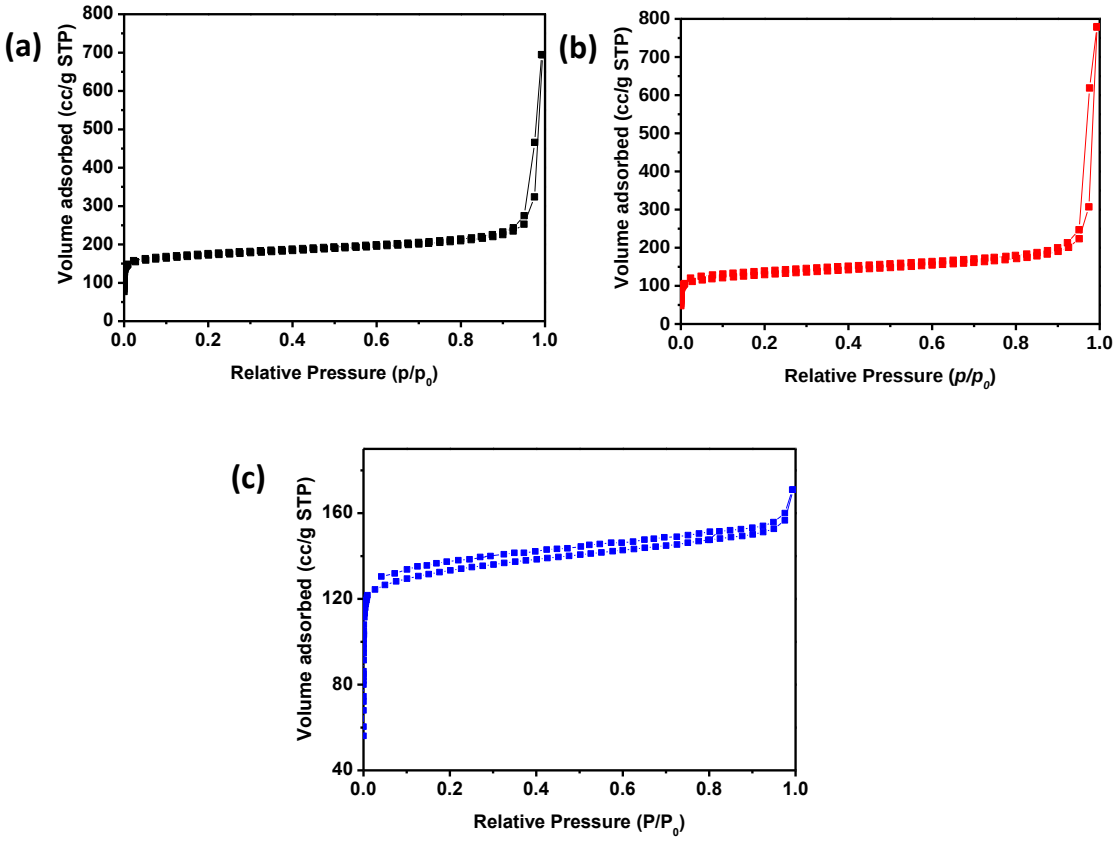


Fig. S26: $N_2$ adsorption-desorption isotherms of porous carbon nanospheres after MB adsorption: (a) CF108-M, (b) CF127-M and (c) CL64-M.

Table S1: Parameters of kinetic models for the adsorption of phenol and MB

| Sample ID | Kinetic Model | Adsorption of phenol | | |
|---|---|---|---|---|
| | | $K_1$ ($min^{-1}$) | | $R^2$ |
| CF108 | Pseudo-first order | 0.454 | | 0.984 |
| CF127 | | 0.101 | | 0.890 |
| CL64 | | 0.180 | | 0.900 |
| | | Adsorption of MB | | |
| CF108 | | 0.731 | | 0.888 |
| CF127 | | 0.360 | | 0.923 |
| CL64 | | 0.100 | | 0.963 |
| | Pseudo-second order | Adsorption of phenol | | |
| | | $q_e$ (mg/g) | $K_2$ ($gmg^{-1}min^{-1}$) | $R^2$ |
| CF108 | | 9.4 | 0.905 | 0.999 |
| CF127 | | 9.0 | 0.114 | 0.997 |
| CL64 | | 7.9 | 0.073 | 0.992 |
| | | Adsorption of MB | | |
| CF108 | | 3.2 | 19.53 | 0.998 |
| CF127 | | 3.196 | 8.158 | 0.999 |
| CL64 | | 2.768 | 1.517 | 0.994 |

Table S2: Parameters obtained from Langmuir, Freundlich and Temkin using different adsorbate concentration

| Sample ID | Adsorption of phenol | | | | Adsorption of MB | | | |
|---|---|---|---|---|---|---|---|---|
| | Langmuir | | | | Langmuir | | | |
| | $q_m$(mg/g) | $K_L$(L/mg) | $R^2$ | | $q_m$ (mg/g) | $K_L$ (L/mg) | $R^2$ | |
| CF108 | 99 | 1.09 | 0.986 | | 68.49 | 0.88 | 0.996 | |
| CF127 | 94.25 | 0.43 | 0.964 | | 30.86 | 1.27 | 0.998 | |
| CL64 | 75 | 0.12 | 0.676 | | 20.83 | 0.51 | 0.977 | |
| | Freundlich | | | | Freundlich | | | |
| | $n_F$ | $K_F$ | $R^2$ | | $n_F$ | $K_F$ (mg/g) | $R^2$ | |
| CF108 | 6.45 | 58.32 | 0.569 | | 3.00 | 26.77 | 0.982 | |
| CF127 | 3.72 | 38.86 | 0.499 | | 5.84 | 17.83 | 0.687 | |
| CL64 | 1.92 | 13.46 | 0.306 | | 4.38 | 9.53 | 0.131 | |
| | Temkin | | | | Temkin | | | |
| | $A_T$ (L/mg) | $b_T$ | $B$ | $R^2$ | $A_T$ (L/mg) | $b_T$ | $B$ | $R^2$ |
| CF108 | 558.84 | 253.9 | 9.92 | 0.500 | 0.089 | 42.1 | 59.79 | 0.778 |
| CF127 | 10.42 | 155.8 | 16.16 | 0.470 | 161.92 | 688.1 | 3.66 | 0.795 |
| CL64 | 0.843 | 102.3 | 24.61 | 0.303 | 102.53 | 1012.5 | 2.48 | 0.161 |

Table S3: Surface area of porous carbon nanospheres after phenol and MB adsorption

| Sample | Surface area ($m^2g^{-1}$) | | |
|---|---|---|---|
| | $S_{BET}$ | $S_{micropore}$ | $S_{mesopore}$ |
| CF108-P | 568.6 | 308.9 | 259.7 |
| CF127-P | 439.0 | 159.9 | 279.1 |
| CL64-P | 438 | 375.5 | 62.45 |
| CF108-M | 602.4 | 347.5 | 254.9 |
| CF127-M | 467.2 | 162.6 | 304.6 |
| CL64-M | 486.8 | 423.4 | 63.4 |